Published online 8 November 2010 *Nucleic Acids Research, 2011, Vol. 39, No. 5* ***1703–1717***
doi:10.1093/nar/gkq1031

A prominent β-hairpin structure in the winged-helix domain of RECQ1 is required for DNA unwinding and oligomer formation

Bojana Lucic[1], Ying Zhang[2], Oliver King[2], Ramiro Mendoza-Maldonado[1], Matteo Berti[1], Frank H. Niesen[2], Nicola A. Burgess-Brown[2], Ashley C. W. Pike[2], Christopher D. O. Cooper[2], Opher Gileadi[2] and Alessandro Vindigni[1,*]

[1]International Centre for Genetic Engineering and Biotechnology, Padriciano 99, 34149 Trieste, Italy and [2]Structural Genomics Consortium, Old Road Campus Research Building, Roosevelt Drive, University of Oxford, Oxford OX3 7DQ, UK

Received July 20, 2010; Revised October 6, 2010; Accepted October 8, 2010

ABSTRACT

RecQ helicases have attracted considerable interest in recent years due to their role in the suppression of genome instability and human diseases. These atypical helicases exert their function by resolving a number of highly specific DNA structures. The crystal structure of a truncated catalytic core of the human RECQ1 helicase (RECQ1$^{49–616}$) shows a prominent β-hairpin, with an aromatic residue (Y564) at the tip, located in the C-terminal winged-helix domain. Here, we show that the β-hairpin is required for the DNA unwinding and Holliday junction (HJ) resolution activity of full-length RECQ1, confirming that it represents an important determinant for the distinct substrate specificity of the five human RecQ helicases. In addition, we found that the β-hairpin is required for dimer formation in RECQ1$^{49–616}$ and tetramer formation in full-length RECQ1. We confirmed the presence of stable RECQ1$^{49–616}$ dimers in solution and demonstrated that dimer formation favours DNA unwinding; even though RECQ1 monomers are still active. Tetramers are instead necessary for more specialized activities such as HJ resolution and strand annealing. Interestingly, two independent protein–protein contacts are required for tetramer formation, one involves the β-hairpin and the other the N-terminus of RECQ1, suggesting a non-hierarchical mechanism of tetramer assembly.

INTRODUCTION

Since the discovery of the first RecQ enzyme from *Escherichia coli* over 20 years ago (1), numerous other RecQ family helicase genes have been found in various organisms ranging from prokaryotes to eukaryotes. Unicellular organisms, such as bacteria and yeast have only one or two RecQ helicase genes per species, while higher eukaryotes generally express multiple RecQ enzymes (2–4). Five members of the RecQ family have been found in human cells: BLM, RECQ1 (*alias* RECQL or RECQL1), RECQ4 (RECQL4), RECQ5 (RECQL5) and WRN. Mutations in the genes encoding BLM, WRN and RECQ4 are linked to defined genetic disorders associated with genomic instability, cancer predisposition and features of premature aging (5–9). No heritable cancer predisposition disorder has been associated with mutations in the remaining two human RecQ helicase genes, *RECQ1* and *RECQ5* as yet. However, recent studies have linked a single-nucleotide polymorphism present in the *RECQ1* gene to a reduced survival in pancreatic cancer patients (10). Recent reports showing that RECQ1 silencing has anti-cancer effect both in cellular and mouse xenograft models suggest that RECQ1 may have a role in cancer survival, and might be considered as a new suitable target for cancer therapy (11–13).

RecQ helicases unwind DNA with a 3′–5′ polarity and are capable of unwinding a variety of DNA structures in addition to standard B-form DNA duplexes, i.e. triple helices, 3- or 4-way junctions, and G-quadruplex DNA (14–17). Consistent with an ability to unwind various DNA structures, several cellular functions have been

*To whom correspondence should be addressed. Tel: +39 040 3757326; Fax: +39 040 226555; Email: vindigni@icgeb.org

© The Author(s) 2010. Published by Oxford University Press.
This is an Open Access article distributed under the terms of the Creative Commons Attribution Non-Commercial License (http://creativecommons.org/licenses/by-nc/2.5), which permits unrestricted non-commercial use, distribution, and reproduction in any medium, provided the original work is properly cited.

attributed to RecQ proteins, including roles in stabilization and repair of damaged DNA replication forks, telomere maintenance, homologous recombination and DNA damage checkpoint signaling (2,3,18). RECQ1 was the first RecQ helicase to be discovered in humans on the basis of its potent ATPase activity (19), but it is one of the less characterized in terms of enzymatic activity and function. Our previous studies demonstrated that RECQ1 has a substrate specificity that is distinct from that of BLM and WRN, suggesting that these helicases play non-overlapping functions in cells and that there must be key structural features that distinguish the catalytic domains of these enzymes (20). Of note, the substrate specificity of RECQ1 is also different from that of *E. coli* RecQ; for example, RECQ1 cannot resolve blunt-ended DNA duplexes or G-quadruplex DNA, both of which are efficiently unwound by the bacterial helicase.

Recently, a truncated form of RECQ1 lacking the first 48 residues and the last 33 amino acids at the C-terminus ($RECQ1^{49–616}$) was crystallized in presence of $MgCl_2$ and ATPγS, and its structure was determined at a resolution of 2.0 Å (21). The truncated protein $RECQ1^{49–616}$ has an activity very similar to the full-length RECQ1 on a forked-duplex substrate, hence it can be seen as the catalytic core [similar to the crystallized fragment of the *E. coli* enzyme (22)]. However, it has no detectable strand annealing activity, consistent with our previous observation that higher order oligomers are responsible for strand annealing and that the N-terminus is required for higher order oligomer formation (20,23). Moreover, the N-terminally deleted mutant lacks Holliday junction (HJ) disruption activity, suggesting that the N-terminal domain, either directly or through the formation of higher order oligomers, is essential for the ability of RECQ1 to disrupt HJs (20).

A distinguishing feature of RecQ helicases is a RecQ-specific C-terminal domain (RecQ-Ct), which consists of a zinc-binding module and a winged-helix (WH) domain (24). The WH domains of *E. coli* RecQ, and the human RECQ1 and WRN helicases are structurally similar; however, the structures of *E. coli* RecQ and human RECQ1 differ in the orientation of the WH relative to the other helicase domains. In addition, human RECQ1 shows a prominent β-hairpin, with a tyrosine residue (Y564) at the tip, located in the wing of the WH domain. The corresponding β-hairpin in WRN is similarly topped by a phenylalanine at the same position; in contrast, the β-hairpin is much shorter and lacks an aromatic residue in the structure of the winged-helix (WH) domain of *E. coli* RecQ. Our previous mutagenesis studies indicated that this hairpin plays a crucial role in the DNA strand separation activity of $RECQ1^{49–616}$, as all mutants of the β-hairpin, including the single amino acid change of the aromatic residue at the tip (Y564A), are nearly devoid of DNA unwinding activity (21). These results suggest that the Tyr residue may act as a pin that abuts the end of the DNA duplex and hence promotes strand separation. A similar role has been previously ascribed to unrelated β-hairpin structures in other helicases of both the SF-1 and SF-2 superfamilies (25).

Here, we further investigated the contribution of the β-hairpin to the enzymatic activity of RECQ1 in the context of the full-length protein. Our mutational and structural data point to an additional role of the β-hairpin as an important interface for oligomer formation, and identify the distinct roles of different RECQ1 subunit interfaces in the formation of dimers and tetramers. Collectively, these studies provide new insight into the mechanism that regulates higher assembly state formation and controls the balance between the multiple enzymatic activities of RECQ1.

MATERIALS AND METHODS

Proteins

Full-length RECQ1 ($RECQ1^{FL}$) and its mutants were purified from baculovirus/Sf9 cells as described previously (23,26). The truncated form of RECQ1 lacking the first 48 residues at the N-terminus and the last 33 amino acids at the C terminus ($RECQ1^{49-616}$, also termed $RECQ1^{T1}$) and its mutants were instead produced in *E. coli* following a previously described procedure (21).

DNA substrates

All oligonucleotides were chemically synthesized and purified by reverse-phase high pressure liquid chromatography (RP-HPLC) (Sigma-Aldrich, Suffolk, UK). Each nucleotide was then resuspended in Tris–EDTA (TE) buffer (10 mM Tris–HCl, pH 7.5, 1 mM EDTA, pH 8.0). Oligonucleotide sequences used in helicase and annealing assays are reported in Table 1. For each substrate, a single oligonucleotide was 5′-end-labeled with [γ-^{32}P] ATP using T4 polynucleotide kinase. The kinase reaction was performed in PNK buffer (70 mM Tris–HCl, pH 7.6, 10 mM $MgCl_2$, 5 mM dithiothreitol) at 37°C for 45 min.

Table 1. Sequences of oligonucleotides used for substrate preparation

Oligonucleotide		
Number	Name	Sequence 5′–3′
1	Fork 20 (D)	GAACGAACACATCGGGTACGTTTTTTTTTTTTTTTTTTTTTTTTTTTTTT
2	Fork 20 (U)	TTTTTTTTTTTTTTTTTTTTTTTTTTTTTTTCGTACCCGATGTGTTCGTTC
8	X12-1	GACGCTGCCGAATTCTGGCTTGCTAGGACATCTTTGCCCACGTTGACCCG
9	X12-2	CGGGTCAACGTGGGCAAAGATGTCCTAGCAATGTAATCGTCTATGACGTC
10	X12-3	GACGTCATAGACGATTACATTGCTAGGACATGCTGTCTAGAGACTATCGC
11	X12-4	GCGATAGTCTCTAGACAGCATGTCCTAGCAAGCCAGAATTCGGCAGCGTC

For helicase assays, the [γ-^{32}P]ATP-labeled oligonucleotides were then annealed to a 1.6-fold excess of the unlabeled complementary strands in annealing buffer (10 mM Tris–HCl, pH 7.5, 50 mM NaCl) by heating at 95°C for 8 min and then cooling slowly to room temperature. The purification of the forked duplex substrates was performed using Micro Bio-Spin columns (Bio-Rad), while the HJ substrates were purified using Sepharose-4B columns (Amersham Biosciences).

Helicase assay

Helicase assays were performed in 20 µl of a reaction mixture containing helicase buffer (20 mM Tris–HCl, pH 7.5, 8 mM dithiothreitol, 5 mM $MgCl_2$, 10 mM KCl, 10% glycerol, 80 µg/ml bovine serum albumin), 5 mM ATP and [γ-^{32}P] ATP-labeled fork or synthetic HJ substrate (0.5 nM). The reactions were started by the addition of recombinant RECQ1 proteins (or its mutants) to a concentration indicated in the figures, and the mixture was incubated at 37°C for 20 min. The reactions were terminated by the addition of 20 µl of quench solution (0.4 M EDTA pH 8.0, 1% SDS, 10% glycerol). Reaction products were resolved using 10% native PAGE and the extent of DNA unwinding was quantified as described previously (26).

DNA binding assay

The DNA binding assays where performed by EMSA using the fork duplex and HJ substrates (Table 1). Briefly, the experiments were performed by incubating increasing concentrations of the purified protein (0–200 nM) with [γ^{32}-P] labeled DNA (0.5 nM) in a 20 µl reaction mixture containing 20 mM Tris–HCl pH 7.8, 2 mM $MgCl_2$, 50 mM NaCl, 1 mM DTT and 0.1 mg/ml BSA. After incubation for 30 min at room temperature, 2.5 µl of 30% glycerol were added and the reaction products were separated on a 6% non-denaturing polyacrylamide gel run at 4°C in TBE buffer. Labeled DNA fragments were detected by autoradiography (Cyclon, GE Healthcare). The apparent equilibrium dissociation constant (K_d) was determined from the mean of at least three independent experiments.

Size exclusion chromatography experiments

Size exclusion chromatography experiments were performed on a ÄKTA FPLC system (Amersham Biosciences) using a 10/30 Superdex 200 HR gel filtration column (GE Healthcare), as described previously (23). Briefly, the column was equilibrated at a flow rate of 0.5 ml/min with 20 mM Tris (pH 7.5), 150 mM KCl and 1 mM DTT. Approximately 150–200 µg of recombinant protein was loaded on the column and detected using an UV detector at 280 nm.

Analytical ultracentrifugation

Sedimentation velocity experiments were carried out at 8°C on a Beckman XL-I analytical ultracentrifuge equipped with a Ti-50 rotor. Protein samples were studied at a concentration of 0.5 mg/ml (or a mixture of two proteins, each at 0.5 mg/ml) in 10 mM HEPES pH 7.4, 150 mM NaCl, 0.5 mM TCEP, 2% (v/v) glycerol. After equilibration at 8°C for 1 h, 3000 r.p.m., the speed was increased to 50 000 r.p.m. for RECQ1^{T1} or 40 000 r.p.m. for RECQ1^{FL}, and radial absorbance scans were taken every 2 min at 280 nm. Information from scans 5–50 was used for analysis. Data were analyzed using SEDFIT (27) to calculate c(s) distributions. The software package SEDNTERP (http://www.jphilo.mailway.com) was used in order to normalize the obtained sedimentation coefficient values to the corresponding values in water at 20°C, $s^0_{20,w}$.

Analytical ultracentrifugation (AUC) sedimentation equilibrium experiments were performed at 8°C, with protein concentrations of 0.5, 0.3 and 0.2 mg/ml, dialysed against 10 mM HEPES pH 7.4, 150 mM NaCl, with addition of 1.0 mM TCEP. The samples were centrifuged at 7000 r.p.m. for 22 h and scanned; a further scan after 2 h was performed to confirm that equilibrium had been attained. The speed was then increased to 9000 r.p.m., and the chambers were scanned after 18 and 20 h. Finally, the speed was increased to 26 000, to achieve meniscus depletion, providing a baseline for the analysis.

Dynamic light scattering

The dynamic light scattering (DLS) measurements were carried out at 20°C at a scattering angle of 90° (Model 802 DLS, Viscotek, correlator resolution = 256 channels). A 12–µl cuvette was filled with 1 mg/ml of each sample in a buffer comprising 10 mM HEPES, pH 7.5, 150 mM NaCl, 2% (v/v) glycerol, after filtration (200 nm, NanoSep, Pall). Of each sample, at least 30 autocorrelations (duration: 2 s) were collected. A minimum of 10 similar autocorrelations representing the average were used to fit for the distribution of particles according to their hydrodynamic radius, $N(R_h)$, from Laplace inversion (OmniSIZE, Viscotek), applying a buffer viscosity of 0.010825 poise, as calculated using SEDNTERP.

GST pull-down assay

We produced [^{35}S]-labeled RECQ1 for in vitro binding assays by the TNT Reticulocyte Lysate System (Promega), using the corresponding pIRES FLAG-Hemagglutinin (FH)-RECQ1 vector as template. Glutathione S-transferase (GST) and GST-fused wild-type and truncated RECQ1 proteins were expressed in bacteria and purified according to a previously described procedure (28). Briefly, bacterial cultures harboring GST-fused proteins were induced with 1 mM isopropyl-β-D-thiogalactopyranoside (IPTG) over night at room temperature. The pellets were resuspended in lysis buffer (50 mM Tris–HCl pH 8.0, 250 mM NaCl, 5% glycerol, 5 mM EDTA, 2 mM DTT and 1 mM PMSF plus protease inhibitor cocktail tablet) and sonicated. The cleared lysates were then loaded onto glutathione agarose beads (Sigma) and incubated for 1 h at 4°C. Following incubation and extensive washing with lysis buffer, proteins immobilized on beads were resuspended at 50% (v/v) in the same buffer and kept frozen until use. GST pull-down assays were performed as described (28,29). Briefly, immobilized

GST-fused RECQ1 fragments were pretreated with DNase I and RNase A for 30 min at 25°C to remove bacterial nucleic acids. The beads were then washed twice with high salt solution (1 M NaCl) and equilibrated in binding buffer TNEN [20 mM Tris–HCl (pH 7.5), 150 mM NaCl, 1.0 mM EDTA pH 8.0, 0.5 % NP-40, 1 mM DTT 1, mM PMSF] supplemented with 0.1 mg/ml of ethidium bromide. The labeled *in vitro* translated RECQ1 protein was then added to 1–5 μg of proteins immobilized on beads in the same buffer in a final volume of 50 μl. The reaction mixture was incubated for 2 h at 4°C. The beads were subsequently washed two times in the ethidium bromide supplemented TNEN buffer, and three times with TNEN buffer. Finally, the beads were resuspended, heated in Laemmli buffer and separated by SDS–PAGE. Dried gels were visualized with a Phosphoimager. The two bands visible on the gels for the *in vitro* translated RECQ1 protein represent two protein products derived from two alternative translation initiation ATG codons. The first codon is located 'upstream' of FLAG-Hemagglutinin double tag, while the second corresponds to the ATG initiation codon of RECQ1 located 'downstream' of the double tag.

RESULTS

The β-hairpin of RECQ1^{FL} is required for fork duplex unwinding and HJ branch migration

We have previously identified an essential role for the β-hairpin located in the WH domain in the forked-duplex DNA strand-separation activity of the truncated form of the RECQ1 protein (RECQ1$^{49\text{-}616}$). This truncated protein will be termed RECQ1^{T1} for simplicity (21). Here, we tested the impact of similar β-hairpin mutations on the ability of the full-length RECQ1 protein (RECQ1^{FL}) to resolve forked and HJ substrates. In particular, we engineered a point mutant where Tyr564 was replaced with Ala (Y564A-RECQ1^{FL}) and a deletion mutant lacking eight residues on both strands of the β-hairpin in addition to the Y564A substitution (Δ8-Y564A-RECQ1^{FL}) (Table 2). Both proteins were expressed in SF9 cells and purified to near homogeneity using a previously established procedure (Figure 1A) (23,26). Using the mutant protein, we confirmed that the single amino acid substitution of the aromatic residue at the tip of the hairpin (Y564A) significantly affected the ability of RECQ1 to resolve a forked duplex substrate of 20 bp with ssDNA tails of 30 nt, as >95% of the substrate was unwound within 20 min using 10 nM RECQ1^{FL}, while <40% is resolved using the same concentration of the Y564A-RECQ1^{FL} mutant (Figure 1B and C). Interestingly, a more pronounced effect of the same mutation was observed using the HJ substrate since only a very limited amount of the splayed arm product (<15%) was observed using the Y564-RECQ1^{FL} mutant even in the presence of 50 nM enzyme (Figure 1D and E). Deletion of the eight residues on both strands of the hairpin coupled to the replacement of Y564 with alanine had an even more dramatic effect since no unwinding of either DNA substrate was detected even at the highest protein concentrations. Collectively, these results confirm that the Tyr residue at the tip of the hairpin is a crucial structural determinant for the unwinding activity of RECQ1 also in the context of the full-length protein.

Table 2. Hairpin mutants of full-length and truncated human RECQ1

Mutants	Hairpin sequence
Full-length RECQ1 (RECQ1^{FL})	
RECQ1^{FL}	^{554}YLKEDYSFTA**Y**ATISYLKIG^{573}
Y564A-RECQ1^{FL}	^{554}YLKEDYSFTA**A**ATISYLKIG^{573}
Δ8-Y564A-RECQ1^{FL}	^{554}Y AA G^{573}
Truncated RECQ1$^{49–616}$ (RECQ1^{T1})	
RECQ1^{T1}	^{554}YLKEDYSFTA**Y**ATISYLKIG^{573}
Y564A-RECQ1^{T1}	^{554}YLKEDYSFTA**A**ATISYLKIG^{573}
Δ2-Y564A-RECQ1^{T1}	^{554}YLKEDYS AA ISYLKIG^{573}
Δ3-Y564A-RECQ1^{T1}	^{554}YLKEDY AA SYLKIG^{573}
Δ8-Y564A-RECQ1^{T1}	^{554}Y AA G^{573}
Δ(F561-T562-T566)-RECQ1^{T1}	^{554}YLKEDYS A**Y**A ISYLKIG^{573}
Y559A-S560A-F561A-RECQ1^{T1}	^{554}YLKED**AAA**TA**Y**ATISYLKIG^{573}
W227A-F231A-RECQ1^{T1}	*(mutations not in hairpin)*

The β-hairpin is involved in RECQ1^{T1} dimer formation

When purifying the β-hairpin mutants of RECQ1^{T1} we noticed that all mutants in which the hairpin was shortened by two or more amino acids on each strand eluted on gel filtration columns later than RECQ1^{T1} (Figure 2A). RECQ^{T1} eluted from the gel filtration column with an apparent molecular mass of ~150 kDa, while the mutants carrying deletions in the β-hairpin eluted with an apparent molecular mass of ~67 kDa. Importantly, the Y564A mutation alone did not cause the same shift. This shift in chromatographic behavior could be due to changes in the conformation or in the oligomeric state of RECQ1^{T1}. To resolve this, both the RECQ1^{T1} protein and the mutant denoted Δ2 (Δ2-Y564A-RECQ1^{T1}), were analyzed by AUC, DLS and chemical cross-linking (Figure 2). The values of the sedimentation coefficients measured by analytical ultracentrifugation for Δ2-Y564A-RECQ1^{T1} and RECQ1^{T1} were 4.0 S and 6.0 S, respectively (Figure 2B). In agreement with the gel filtration profiles, each protein sedimented predominantly as a single peak. These sedimentation coefficients and the estimated diffusion coefficients correspond to molecular masses of 63 kDa and 117 kDa for Δ2-Y564A-RECQ1^{T1} and RECQ1^{T1}, respectively (the molecular mass of a single chain or RECQ1^{T1} is 67.2 kDa). Equilibrium ultracentrifugation was used to calculate masses of 72 kDa and 132 kDa for Δ2-Y564A-RECQ1^{T1} and RECQ1^{T1}, confirming that the two proteins behave as a monomer and a dimer, respectively (Figure 2C). DLS provided separate confirmation that both Δ2-Y564A-RECQ1^{T1} and RECQ1^{T1} proteins were monodisperse, with calculated masses of 67 kDa and 133 kDa, respectively, corresponding to a monomer and dimer (Figure 2D). This conclusion was further supported by chemical cross-linking, that showed a cross-linked species of double molecular weight for RECQ1^{T1}, but not for Δ2-Y564A-RECQ1^{T1} (Figure 2E). Collectively, these experiments indicate that

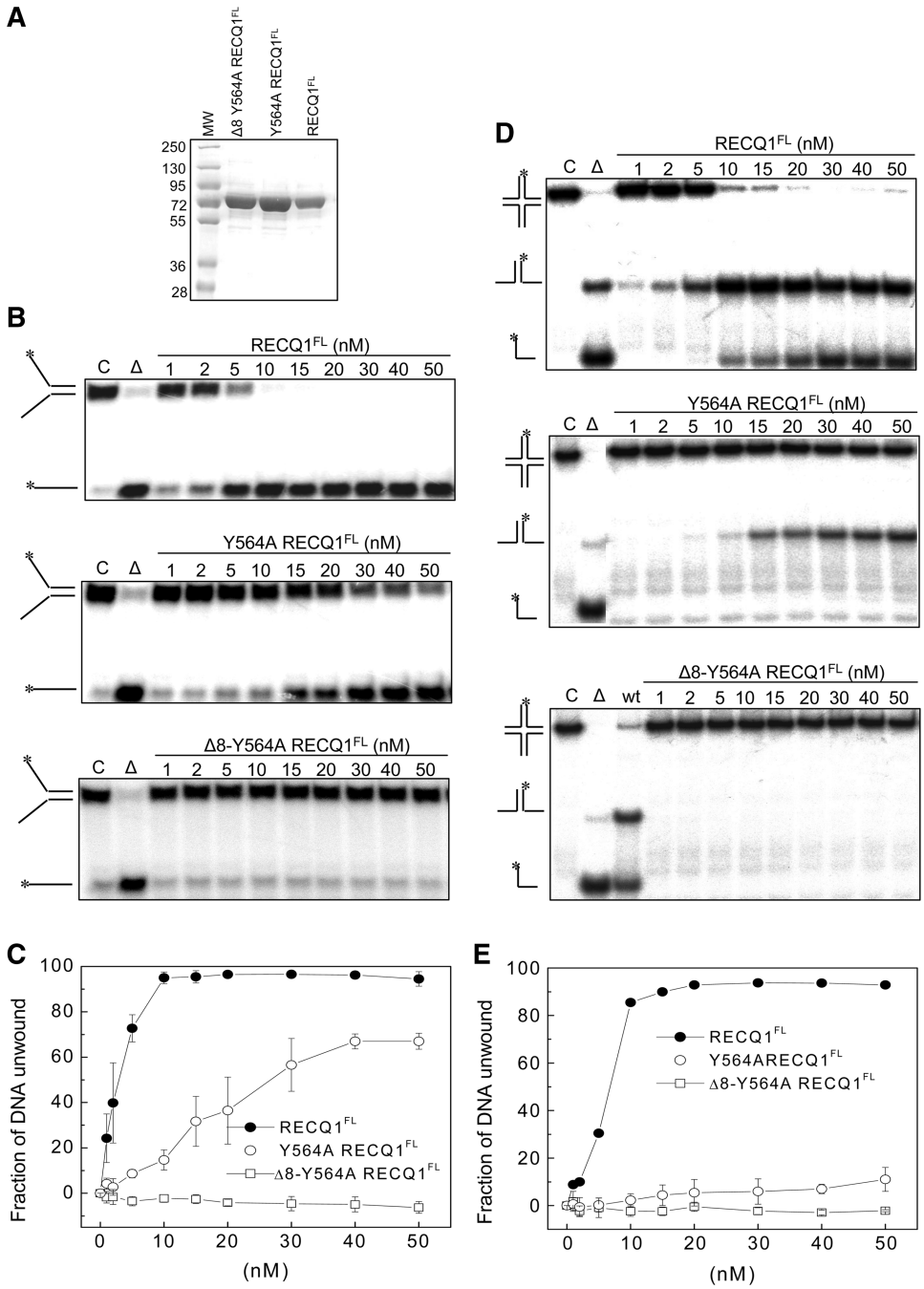

Figure 1. Analysis of the unwinding activity of hairpin loop mutants of full-length RECQ1. (**A**) SDS–PAGE analysis of the purified RECQ^{FL}, Y564A-RECQ1^{FL} and Δ8-Y564A-RECQ1^{FL} proteins. (**B**) Unwinding assays using various concentrations of RECQ1^{FL}, Y564A-RECQ1^{FL} and Δ8-Y564A-RECQ1^{FL} (0–50 nM) and a forked-duplex substrate of 20 bp with ssDNA tails of 30 nt (0.5 nM). All of the reactions were stopped after 20 min. (**C**) Plot of the unwinding activity as a function of protein concentration using the forked-duplex substrate. Concentration dependence experiments were performed using the mutants indicated in the figure (0–50 nM). The data points represent the mean of three independent experiments with the standard deviation indicated by error bars. (**D**) Unwinding assays using various concentrations of RECQ1^{FL}, Y564A-RECQ1^{FL} and Δ8-Y564A-RECQ1^{FL} (0–50 nM) and a HJ substrate with a 12-bp homologous core (0.5 nM). All of the reactions were stopped after 20 min. (**E**) Plot of the unwinding activity as a function of protein concentration using the HJ substrate. Concentration dependence experiments were performed by using the mutants indicated in the figure (0–50 nM). The data points represent the mean of three independent experiments with the standard deviation indicated by error bars.

the RECQ1^{T1} protein is present predominantly as a dimer in solution, whereas the mutants deleted in the β-hairpin are mainly monomers. Furthermore, the similarity of the gel filtration profiles of RECQ1^{T1} obtained in the presence of ATPγS, and/or ssDNA indicated that the oligomeric state of RECQ1^{T1} was not affected by the interaction with a slowly hydrolyzable analog of ATP and/or ssDNA (21).

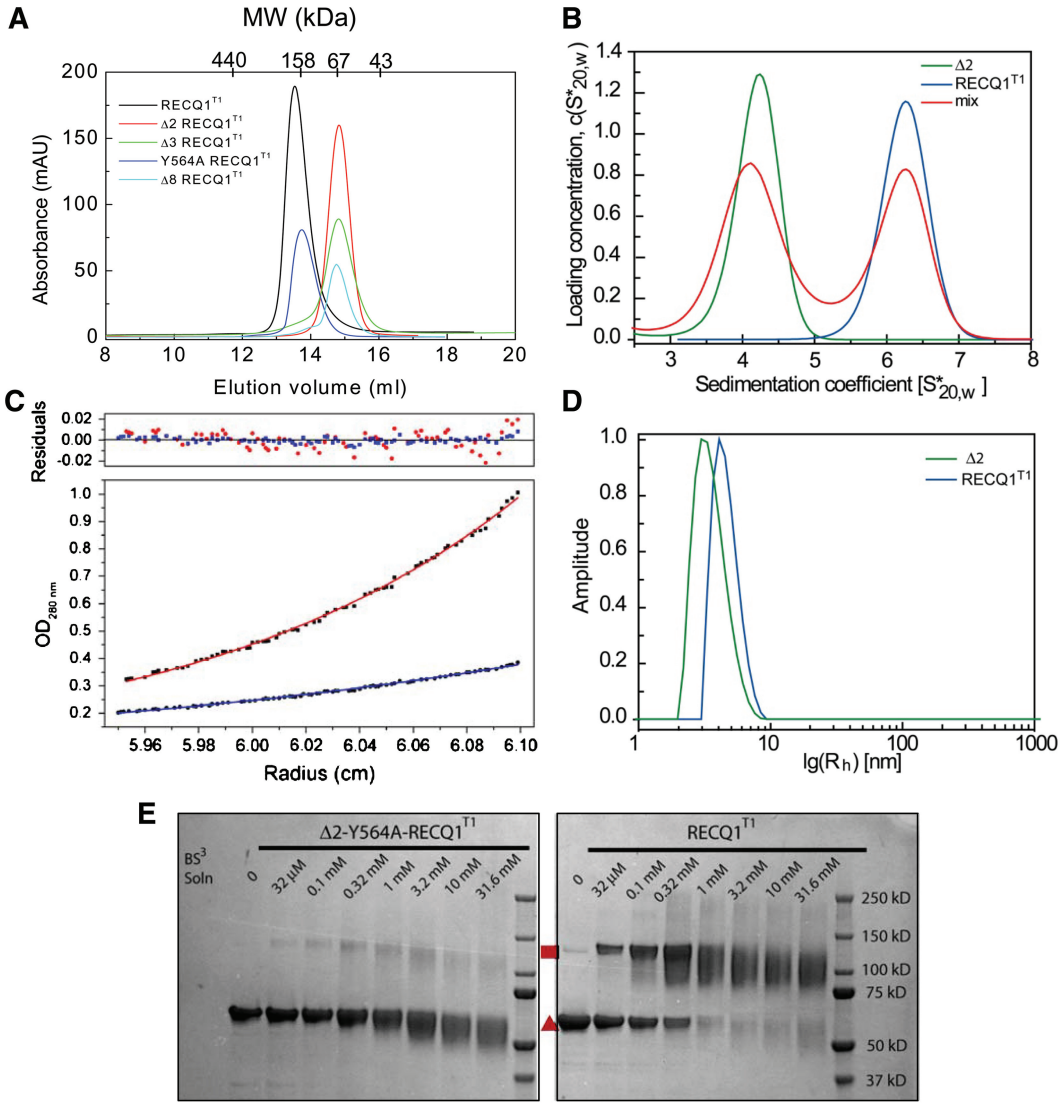

Figure 2. RECQ1^{T1} is a dimer in solution. (**A**) Size exclusion chromatography profiles of RECQ1^{T1} (black), Y564A-RECQ1^{T1} (blue), Δ2-Y564A-RECQ1^{T1} (red), Δ3-Y564A-RECQ1^{T1} (green), Δ8-Y564A-RECQ1^{T1} (cyan). (**B**) Sedimentation velocity in AUC. Blue: RECQ1^{T1}, green: Δ2-Y564A-RECQ1^{T1} mutant, red: 1:1 mixture of both proteins. (**C**) Absorbance distribution for RECQ1^{T1} in sedimentation equilibrium experiments shows dimerization. The ideal fit curves of both proteins at 9000 r.p.m. The red curve is an ideal fit of the data for RECQ^{T1}, giving a molecular weight of 132 kDa; the blue curve is an ideal fit for the Δ2-Y564A- RECQ1^{T1} mutant, giving a MW of 72 kDa. The residuals of both datasets are shown in the upper panel, showing absence of either aggregation or non-ideality. (**D**) Size distributions investigated with dynamic light scattering. The monodisperse distribution of RECQ1^{T1} (blue trace) shows a hydrodynamic radius equivalent to a mass of 133 kDa (calculated monomolecular weight: 67.3 kDa). The hydrodynamic radius observed for the Δ2-Y564A-RECQ1^{T1} mutant (green trace) was equivalent to a mass of 67 kDa (calculated monomolecular weight: 66.8 kDa). (**E**) Protein cross-linking. RECQ1^{T1} (right) and the Δ2-Y564A-RECQ1^{T1} mutant (left) were incubated with the crosslinker BS3 at the indicated concentrations for 30 min. The reactions were quenched and the proteins separated by denaturing SDS–PAGE. Monomers (red triangle) and cross-linked dimers (red square) are indicated.

Our analysis of the crystal structure of RECQ1^{T1} (21) for potential oligomeric assemblies using the PISA server (30) revealed a significant interface with a neighboring molecule in the crystal lattice (Figure 3A). This dimeric interaction results in the burial of 1100 Å^2 of accessible surface area from each monomer, which represents 4.7% of the available surface area. In contrast, all other crystal contacts typically involve <400 Å^2 of buried surface. The same dimeric interactions occur in four different crystal forms of RECQ1^{T1} (PDB: 2V1X, 2WWY, and data not shown), in which other crystal contacts are not conserved. The dimer in the crystal structure is arranged in a head to tail organization, in which the main protein contacts are distributed in three patches, which we term C1, C2 and C3 (a list of interacting residues listed in Table 3; Figure 3A and B). C1 includes a patch of residues that are clustered on one face of the RecA-like domain D1; these interact with C3 region of the dimeric partner, which include residues in the C-terminal Zn and WH domains. The C2 region of each subunit, located at the tip of an aromatic-rich loop in domain D1 (31), lies at the centre of the interface and interacts with the same region in the other monomer.

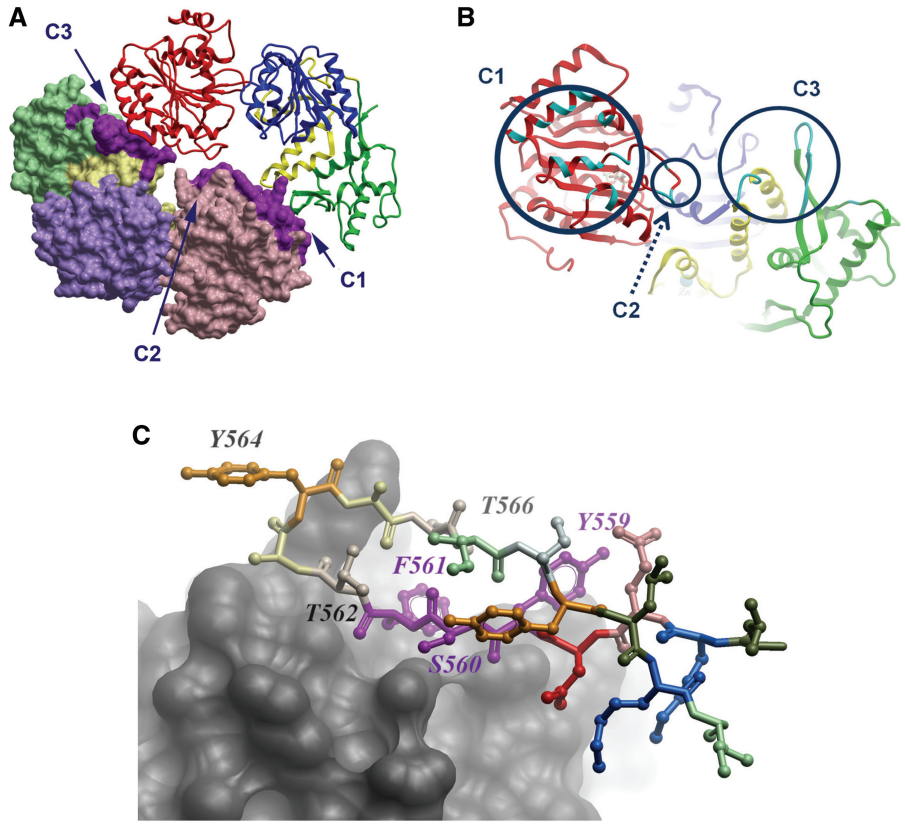

Figure 3. Organization of a RECQ1^{T1} dimer in the crystal structure. (**A**) Overall view, monomer A shown as backbone, monomer B shown in surface representation. The contact areas are indicated in purple. (**B**) The putative dimer interface, on monomer A, from the direction of monomer B. The circles indicate the contact areas C1, C2 and C3; the locations of amino acids involved in the interface are shown in cyan. (**C**) Detailed view of the β-hairpin (ball and stick representation) interacting with the opposing subunit (shown in skin representation). Some of the residues mutated in this study are marked. Specifically, Y559, S560 and F561 are involved in subunit interaction, whereas Y564 and subsequent residues are not directly involved, but are available for potential interaction with DNA.

Interestingly, part of the dimer interface seen in the crystal involves exactly the same residues that are deleted in the hairpin mutants (denoted earlier as C3). Figure 3C shows the interface of the β-hairpin with the adjacent RECQ1 monomer; the most important residues involved in the contact are S560, F561 and T562; the tyrosine at the tip of the hairpin, Y564, plays a lesser role in the subunit interaction. Correspondingly, we found that the Y564A mutation did not disrupt the dimer, but further deletion of F561 caused the dimer to dissociate in solution. This suggests that the dimer interface seen in the crystal structure, or at least the region containing the β-hairpin, is indeed responsible for the dimeric association in solution.

RECQ1^{T1} dimers are not required for DNA unwinding

The fact that RECQ1^{T1} forms dimers in solution and in the crystal structure prompted us to investigate whether dimer formation is required for DNA unwinding. Thus, we engineered new β-hairpin mutants in which some of the key residues involved in the dimer formation were deleted or substituted with alanines, while maintaining the tyrosine residue (Y564) previously shown to be essential for DNA unwinding. In particular, we managed to successfully express and purify a deletion mutant Δ(F561-T562-T566)-RECQ1^{T1} lacking F561 and T562—both of which are involved in the dimer contact—and T566 (the latter was deleted to maintain the equal length of both β-strands of the hairpin). We also expressed the Y559A-S560A-F561A-RECQ1^{T1} mutant, in which three key residues responsible for the contact of the C3 region of one molecule with the C1 region of the other were substituted with Ala (Table 2).

Size exclusion chromatography and chemical cross-linking experiments confirmed that the Δ(F561-T562-T566)-RECQ1^{T1} and Y559A-S560A-F561A-RECQ1^{T1} mutants were monomeric in solution (Figure 4A and B). Moreover, the chemical cross-linking experiments repeated in the presence of ssDNA indicated that these two mutants remained monomeric also in the presence of nucleic acids. The following analysis of the unwinding activity showed that both mutants retained the ability to unwind a forked DNA duplex in a concentration dependent fashion, although they were less active than the dimeric wild-type RECQ1^{T1} (Figure 4C and D). In addition, the Y559A-S560A-F561A-RECQ1^{T1} mutant was more active than Δ(F561-T562-T566)-RECQ1^{T1} possibly because the shortening of the β-hairpin might have affected the ability of Y564 to act as a strand separation pin or the ability of the mutant to interact with DNA.

Table 3. Residues involved in dimer interactions in the crystal structure

Mol1	Mol2
C1	
I194	I194
A195	A195
K198	K198
M199	M199
M201	M201
S202	S202
E205 H	E205 H
–	E209 HS
C2	
Q226	Q226
W227	**W227**
	G228
F231	**F231**
K236	K236
A237	A237
G239	–
I240	I240
R243 H	R243 H
Q244 H	Q244 H
F245	
C3	
E264	
K267 H	
I268 H	I268
C270 H	
V431 H	V431 H
M432	M432
D433	D433
N434	N434 H
K509	
D558	
Y559 H	**Y559 H**
S560 H	**S560 H**
F561 H	**F561 H**
T562	**T562**
A563	**A563**
Y564	**Y564**
A565	**A565**
T566	

The analysis is based on the PISA server (30). The residues that have been mutated or deleted are highlighted in bold. H following the residue number denotes residues involved in interchain hydrogen bonds; S indicates involvement in a salt bridge. The two chains are not symmetry related, and there are slight differences in the pattern of buried residues between the two monomers.

In particular, ~60% of the substrate was unwound by RECQ1^{T1} using 20 nM enzyme, while ~45% unwinding was observed using the same concentration of Y559A-S560A-F561A-RECQ1^{T1} mutant, and this percentage decreased to ~20% using Δ(F561-T562-T566)-RECQ1^{T1}. To test if the reduced unwinding activity of the monomers versus dimers was associated with impairment in DNA binding, we measured the apparent DNA binding affinity of wild-type RECQ1^{T1} and its β-hairpin mutants for the fork-duplex substrate by EMSA. All the β-hairpin mutations, with the notable exception of the Y564A mutation that does not disrupt the dimer interface, affected the DNA binding affinity of the variant proteins (Table 4). Of note, our previous CD spectroscopy and limited proteolysis experiments confirmed that mutations in the β-hairpin do not affect the overall structure of the WH domain (21), thus ruling out the possibility that the reduced DNA binding and unwinding activity is connected to a more extensive destabilization of the WH domain. Collectively, these results indicate that mutant RECQ1^{T1} monomers are still proficient in DNA unwinding, as long as the Y564 is conserved, and that dimers are more active than monomers in DNA unwinding probably because dimer formation provides an additional DNA binding interface that stabilizes the interaction with the substrate.

The aromatic-rich loop of domain D1 is not required for dimer formation, but is essential for DNA unwinding

Our analysis of the crystal structure for additional regions that mediate dimer formation highlighted an aromatic-rich loop in domain D1 which lies at the centre of the interface and interacts with the same region in the other monomer (denoted earlier as C2) (Figure 3B). To test the impact of the C2 region in dimer formation, we expressed an additional mutant W227A-F231A were two aromatic residues involved in protein:protein interactions were substituted with Ala (Table 2). However, our size exclusion chromatography experiments showed that the elution profile did not change significantly relative to wild-type RECQ1^{T1} suggesting that the disruption of the C2 contacts is not sufficient to impair dimer formation (Figure 5A).

Interestingly, this highly conserved aromatic-rich loop was originally identified by Keck and co-workers (31) as essential for DNA-coupled ATP hydrolysis by bacterial RecQ. Consistently, we found that the W227A-F231A mutant was unable to unwind a forked-duplex substrate even at the highest protein concentration used in the experiment (Figure 5B), even though it retained the same DNA binding affinity of wild-type RECQ1^{T1} (Table 4), suggesting that this loop plays an important role in coupling DNA binding to ATP-dependent DNA unwinding also in the case of RECQ1.

The β-hairpin is involved in RECQ1^{FL} higher order oligomer formation

From the comparison of the elution profiles of RECQ1^{T1} and RECQ1^{FL}, and from previous results, we infer that the smallest form of the full-length RECQ1 is also a dimer (21,26). This conclusion was also supported by velocity AUC experiments (Figure 6) confirming that RECQ^{FL} existed as a mix of two oligomeric forms: a smaller form of 140–160 kDa representing RECQ1 dimers, and a 250–280 kDa oligomeric form, which is probably a tetramer, rather than a pentamer or an hexamer as was previously suggested (23). Interestingly, our size exclusion chromatography experiments showed that the β-hairpin Δ8-Y564A-RECQ1^{FL} mutant, that has lost the dimer interface seen in the RECQ^{T1} structure, can still form dimers, but not tetramers (Figure 6A). In line with this observation, our AUC experiments showed that the β-hairpin Δ8-Y564A-RECQ1^{FL} mutant exists in a single form of a dimer, while the Y564A-RECQ1^{FL} is a mixture of dimers and tetramers. The fact that the

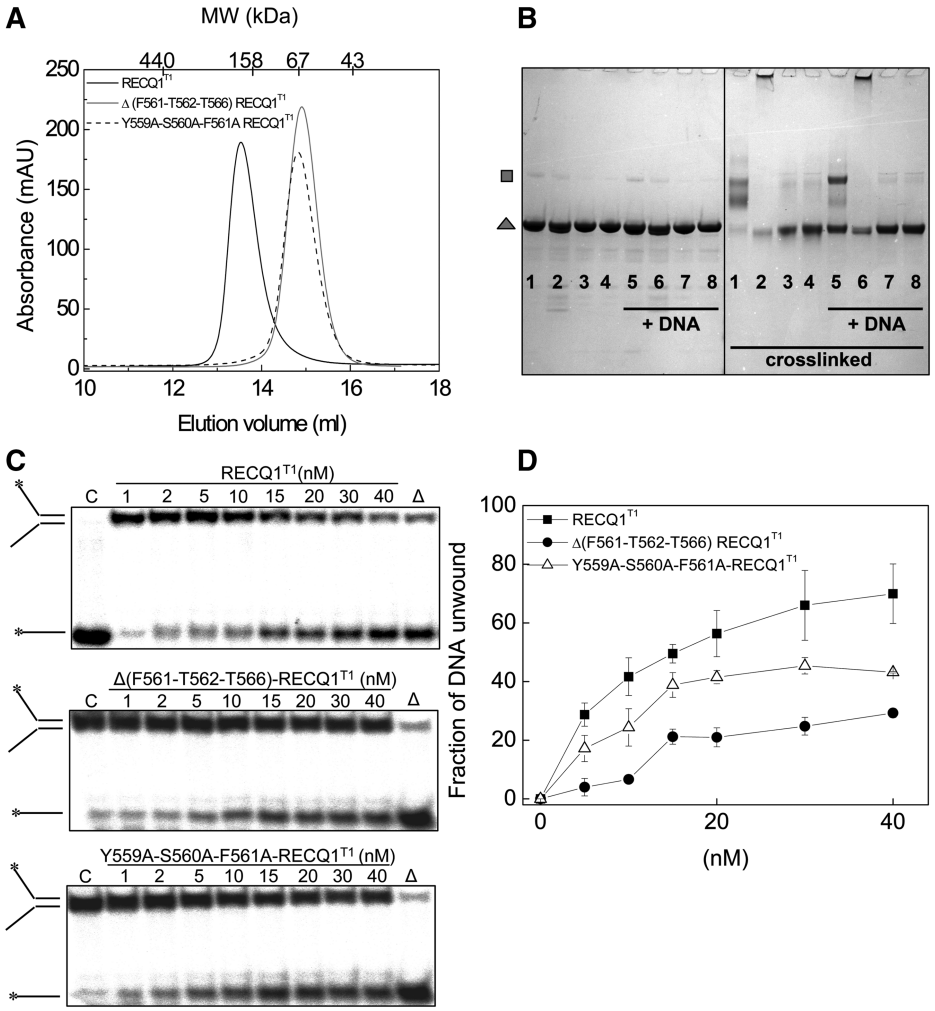

Figure 4. RECQ1^{T1} monomers retain unwinding activity. (**A**) Size exclusion chromatography profiles of RECQ1^{T1}, Δ(F561-T562-T566)-RECQ1^{T1} and Y559A-S560A-F561A-RECQ1^{T1}. (**B**) Cross-linking experiments. Protein samples (10 μM) were incubated with (5–8) or without (1–4) a 42-nt DNA oligonucleotide (50 μM) for 10 min at room temperature. Samples were then treated with the cross-linker BS3 (60 μM, right panel) or control buffer (left panel) for 45 min at room temperature, followed by addition of 100 mM Tris–HCl, pH 7.5, 20 mM TCEP and SDS–PAGE sample buffer. 1, 5: RECQ1^{T1}; 2, 6: Δ2-Y564A-RECQ1^{T1}; 3, 7: Δ(F561-T562-T566)-RECQ1^{T1}; 4, 8: Y559A S560A F561A-RECQ1^{T1}. Monomers (grey triangle) and cross-linked dimers (grey square) are indicated. (**C**) Unwinding assays using various concentrations of RECQ1^{T1}, Δ(F561-T562-T566)-RECQ1^{T1}, and Y559A-S560A-F561A-RECQ1^{T1} (0–40 nM) and a forked-duplex substrate of 20 bp with ssDNA tails of 30 nt (0.5 nM). All of the reactions were stopped after 20 min. (**D**) Plot of the unwinding activity as a function of protein concentration. Concentration dependence experiments were performed using the mutants indicated in the figure (0–40 nM). The data points represent the mean of three independent experiments with the standard deviation indicated by error bars.

Table 4. Summary of the fork–duplex unwinding, HJ branch migration activity and oligomeric properties of all the mutants of RECQ1^{T1} and RECQ1^{FL} tested in this work

Phenotype	RECQ1^{T1}					RECQ1^{FL}		
	Fork unwinding	Fork binding	HJ unwinding	HJ binding	Oligomeric state	Fork unwinding	HJ unwinding	Oligomeric state
Hairpin mutation								
WT	Yes	8 ± 2	No	No	Dimer	Yes	Yes	Dimer + tetramer
Y564A	No	11 ± 2	No	No	Dimer	Partial (50%)	No	Dimer + tetramer
Y564A shortened (Δ2, Δ3, Δ8)	No	>70	No	No	Monomer	No	No	Dimer*
Δ(561–562–566)	Partial (20%)	>70	(*ND*)	No	Monomer	(*ND*)	(*ND*)	(*ND*)
AAA(559–560–561)	Partial (40%)	25 ± 5	(*ND*)	No	Monomer	(*ND*)	(*ND*)	(*ND*)
Aromatic-loop mutation								
AA(227–231)	No	10 ± 2	(*ND*)	No	Dimer	(*ND*)	(*ND*)	(*ND*)

The apparent K_d values (nM) for the binding of RECQ1^{T1} to the fork–duplex substrate are also shown. The asterisk denotes a different kind of dimer held together by the N-terminus of RECQ1.

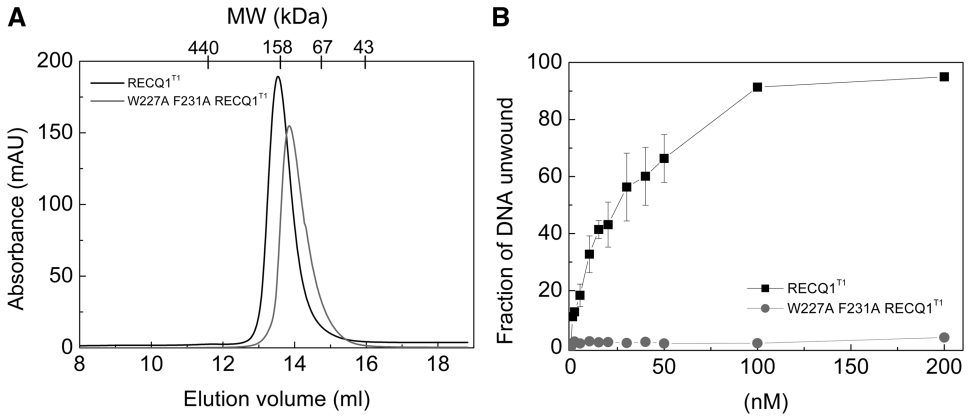

Figure 5. Analysis of the oligomeric properties and unwinding activity of the aromatic-rich loop mutant W227A-F231A-RECQ1^{T1}. (**A**) Size exclusion chromatography profiles of RECQ1^{T1}(black) and W227A-F231A-RECQ1^{T1}(gray). (**B**) Plot of the unwinding activity as a function of RECQ1^{T1} and W227A-F231A-RECQ^{T1} concentration (0–200 nM) using a 20 bp fork-duplex substrate with 30-nt ssDNA tails at a final concentration of 0.5 nM. Reactions were stopped after 20 min. The data points represent the mean of three independent experiments with the standard deviation indicated by error bars.

Δ8-Y564A-RECQ1^{FL} mutant can still form dimers can be explained considering that a protein interaction surface involving the N-terminal residues of RECQ1—which was previously shown to mediate tetramer formation (20,21)—is still functional in the Δ8 mutant that lacks the basic C3 dimer interface formed by the β-hairpin residues.

To map the domains involved in oligomer formation, we tested the ability of the *in vitro* translated RECQ1 protein to interact with a series of GST-tagged RECQ1 fragments mapping the different domains of the protein (Figure 7A). Our GST pull down experiments confirmed that RECQ1^{FL} interacted with the fragment 1–281 containing the N-terminal tail plus domain D1 and with the fragment 391–649 containing the Zn-binding domain and the WH domain where the β-hairpin is located, but not with the fragment 282–390 containing the recA-like domain D2 or with the fragment 391–473 containing the Zn-binding domain alone (Figure 7B). The fragment 474–649 encompassing the WH domain, but lacking the Zn-binding domain, was also able to interact with RECQ1^{FL}, although more weakly compared to fragment 391–649, suggesting that the deletion of residues 391–473 might affect the stability or the conformation of the WH domain. To explore the role of the N-terminus in more detail, we expressed two additional GST-tagged RECQ1 fragments: fragment 1–103 containing the N-terminal tail of RECQ1 and fragment 104–281 encompassing the D1 domain (Figure 7C). The results confirmed that RECQ1^{FL} predominantly interacted with the first 103 aa containing the N-terminal tail previously shown to be involved in oligomer formation (20,21). Collectively, these results confirm that two different regions of RECQ1, the N-terminus and the C-terminal WH domain containing the β-hairpin module, are involved in higher-order oligomer assembly.

DISCUSSION

DNA and RNA helicases and translocases from superfamilies 1 and 2 (SF-1 and SF-2) share a core ATPase domain, which consists of tandem RecA-like folds, and is characterized by conserved sequence motifs (32). In addition to this conserved fold, most helicases include additional loops or domains that are more divergent, and may be conserved only within restricted subfamilies. These non-conserved regions may be important in DNA/RNA unwinding as well as in other enzymatic or regulatory functions. RecQ-family helicases share a characteristic C-terminal domain (termed RecQ-Ct), which includes a zinc-binding module and a WH domain. We have previously suggested, based on structural alignments with other DNA helicases, that the β-hairpin wing of the WH domain is poised to serve as a pin that aids DNA strand separation at a ssDNA–dsDNA junction (21). This prediction was supported by the observation that point mutations or deletions of the hairpin of a truncated form of the RECQ1 protein severely impaired DNA unwinding activity, with no effect on the ssDNA-dependent ATPase activity of the mutant proteins. Here, using β-hairpin mutants of the full-length RECQ1 helicase we show that this prominent β-hairpin is not only essential for fork duplexes unwinding, but it also required the HJ disruption activity of full-length RECQ1, which is one of the most characteristic activities of RecQ proteins (Table 4). In addition, we show that this β-hairpin is a key structural element that controls not only the enzymatic activity of RECQ1, but also the balance between the multiple oligomeric states of the protein. In particular, it mediates dimer formation in the truncated RECQ1 protein lacking 48 residues at the N-terminus and 33 residues at the C-terminus, and tetramer formation in the full-length protein.

Interestingly, a recently published structure of the WH domain of WRN in complex with a 14 base pair DNA duplex shows that the β-hairpin wedges apart the terminal base pair of the DNA duplex, resulting in loss of base–base stacking, thus supporting the notion that the aromatic residue at the tip of the hairpin acts as a pin that abuts the end of the DNA duplex and hence promotes strand separation (33). A recently solved

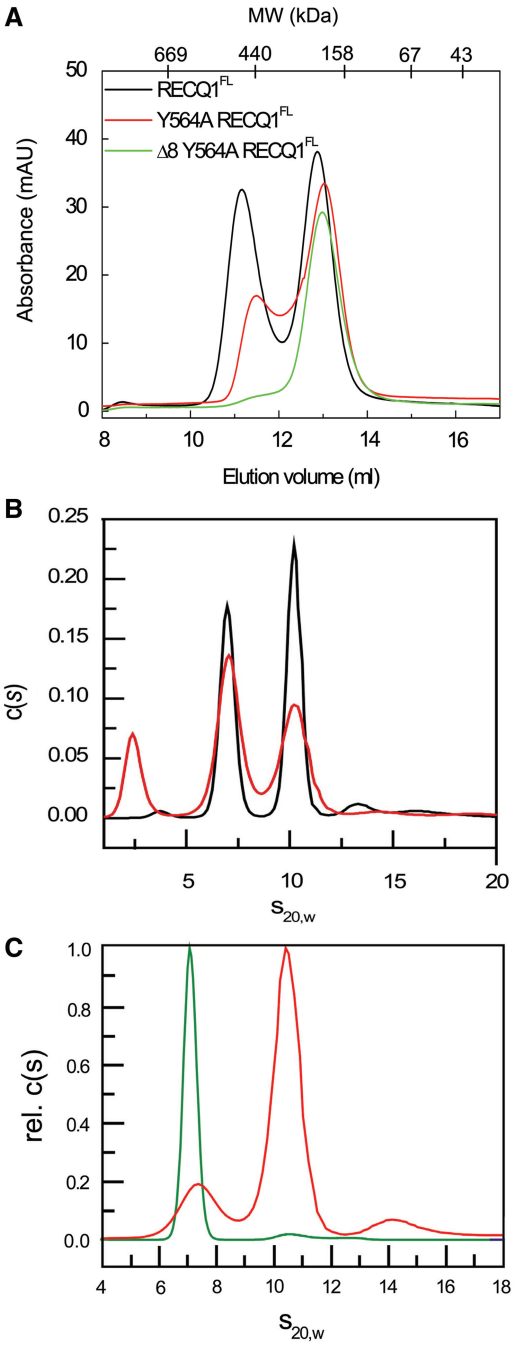

Figure 6. The β-hairpin loop is required for tetramer formation in RECQ1^{FL}. (**A**) Size exclusion chromatography profiles of the purified RECQ^{FL}, Y564A-RECQ1^{FL} and Δ8-Y564A-RECQ1^{FL} proteins. (**B**) Analytical ultracentrifugation of full-length RECQ1. RECQ1^{FL} (subunit MW = 75 620) was analyzed in absence (black curve) or presence (red curve) of 50 μM ATPγS. Two peaks at 7S and 10S correspond to MW of 144 and 260, respectively; a low MW peak seen in the ATPγS experiment may be due to the nucleotide. (**C**) Analytical ultracentrifugation of Y564A-RECQ1^{FL} (red curve) and Δ8-Y564A-RECQ1^{FL} (green curve). The peaks at 7S and 10S correspond to dimers and tetramers; the Y564A-RECQ1^{FL} protein migrates as a mixture of dimers, tetramers and a small amount of higher oligomer or aggregate; the hairpin deletion mutant Δ8-Y564A-RECQ1^{FL}is almost entirely dimeric [note that the *x*-axis in 6A is in order of decreasing size, while the *x*-axes in (B) and (C) represent increasing protein size].

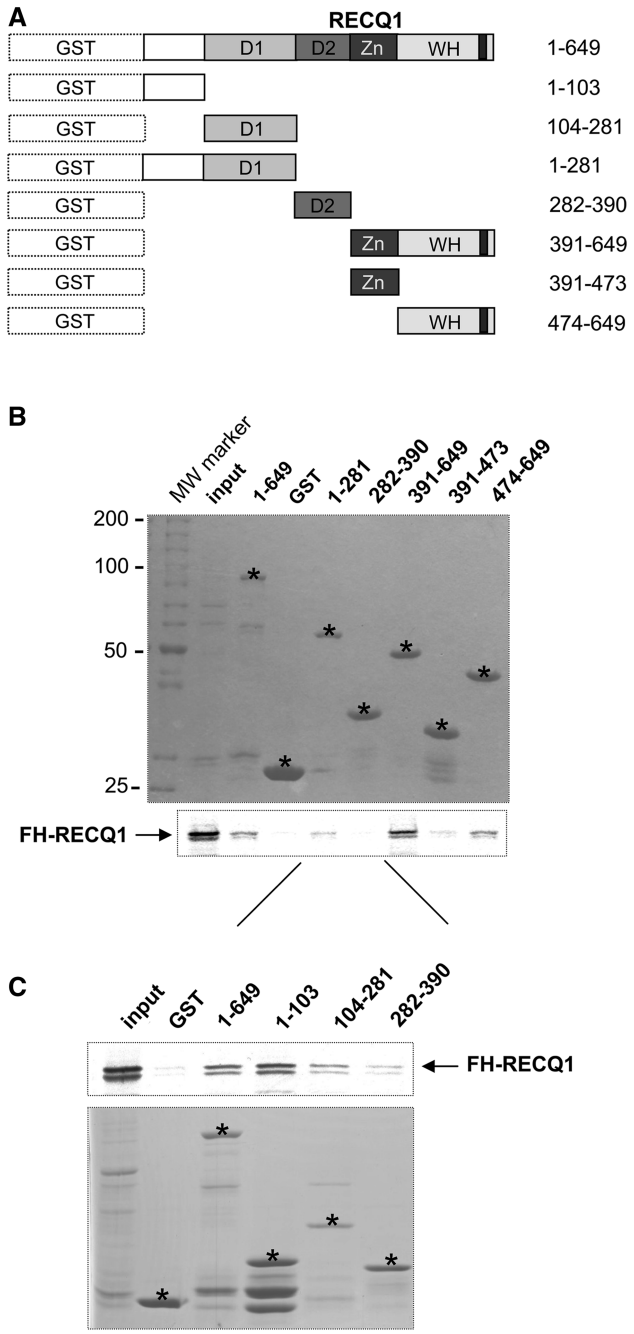

Figure 7. *In vitro* RECCQ1 GST pull-down assay. (**A**) N-terminally GST tagged RECQ1 fragments (aa 1–103, 104–281, 1–281, 282–390, 391–649, 391–473, 474–649) used for the *in vitro* GST pull down assay. (**B**) Top: coomassie stained gel of the GST tagged RECQ1 fragments used in the assay. The stars indicate the location of the fragments in the gels. Bottom: autoradiography of the *in vitro* GST pull-down assay using the ^{35}S-labeled full-length RECQ1 protein. (**C**) Top: autoradiography of the *in vitro* GST pull-down assay using additional GST tagged RECQ1 fragments covering the first 281 aa at the N-terminus of the protein and the ^{35}S-labeled full-length RECQ1 protein. Bottom: coomassie stained gel of the additional GST tagged RECQ1 fragments used in the assay. The stars indicate the location of the fragments in the gels.

structure of a complex of the human RECQ1 with DNA provides further support to this model (PDB ID 2WWY; Pike *et al.*, manuscript in preparation). Similar β-hairpin motifs were previously found to be essential for the unwinding activity of other helicase members of both the SF-1 and SF-2 families. The structures of two SF-1 proteins, UvrD and PcrA, complexed with partial DNA duplexes with 7-nt 3′-tails, show that the bound DNA duplex unwinds in front of a 'pin' located in domain 2A (34,35). Similarly, the crystal structures of the SF-2 proteins, Hel308 from *Archaeoglobus fulgidus* and helicase NS3 of the hepatitis C virus, show a β-hairpin structure between motifs V and VI of the helicase domain (25,36). In particular, the structure of Hel308 bound to a 15-bp DNA duplex with a 10-nt 3′-tail shows that the β-hairpin is positioned exactly at the opening of the unwound tailed duplex (25). Thus, RecQ helicases might share an unwinding mechanism similar to that of these SF-1 and SF-2 helicases where the aromatic residue at the tip of the β-hairpin module sits at junction between ss- and dsDNA, and acts as a 'pin' that promotes strand separation. However, this common structural motif is derived from different regions in the primary structure of SF-1, Hel308 and RECQ1 helicases, and may have evolved independently.

Intriguingly, the β-hairpin is not highly conserved between different RecQ-family proteins (21). In particular, the superimposition of the WH-domain structures of *E. coli* RecQ, RECQ1 and WRN reveals that the β-hairpin is significantly shorter in *E. coli* RecQ and WRN (Figure 8A). Moreover, the aromatic residue at the tip of the β-hairpin of RECQ1 and WRN is substituted with a His in *E. coli* RecQ, suggesting that the β-hairpin module might play different roles in the three helicases. Indeed, we previously showed that a His to Ala substitution at the tip of the hairpin in the bacterial RecQ, as well as deletion of the hairpin, do not affect the enzymatic activity of the bacterial protein (21). The putative β-hairpin in BLM helicase also lacks an aromatic residue. This structural variance indicates that RecQ proteins may utilize different mechanisms for substrate recognition and unwinding.

This apparently straightforward interpretation of the role of the β-hairpin is complicated by our observations on the oligomeric state of RECQ1. The purified full-length RECQ1 protein (denoted here RECQ1^{FL}) occurs as a mixture of a lower and higher oligomeric forms. We here determine, using analytical ultracentrifugation and gel filtration, that these correspond to dimers and tetramers of RECQ1. We have previously observed that deletion of a short amino-terminal segment (aa 1–48) leads to loss of the tetrameric form. A truncated protein (RECQ1^{T1}, lacking the first 48 aa and the last 33 aa at the C-terminus), which purifies uniquely as a dimer, was used in crystallization experiments. The crystal structure identifies a potential dimerization interface between two adjacent RECQ1 molecules. The two molecules in the dimer are arranged in a head to tail orientation. The buried interaction surface may be divided into three patches: an amino-terminal region termed C1 interacts with a C-terminal patch (C3) in the opposite subunit.

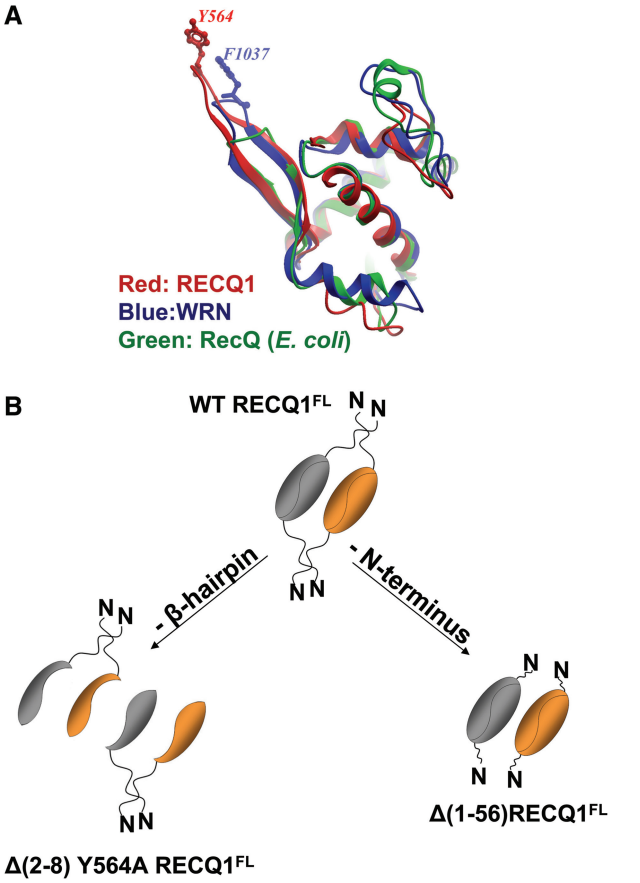

Figure 8. (**A**) Superimposition of WH domains of the RecQ-Ct regions of human RECQ1 (red; 2V1X), *E. coli* RecQ (green; 1OYW) and WRN (blue; 3AAF). The β-hairpins are seen in the upper-left corner. Aromatic residues at the tip of the hairpin (Y564 in RECQ1 and F1037 in WRN) are shown; there is no aromatic residue at the tip of the shorter hairpin of the *E. coli* enzyme. (**B**) Model for RECQ^{FL} tetramer assembly. The RECQ1^{FL} tetramer is represented at the top. Two independent protein–protein contacts are required for tetramer formation, one mediated by the β-hairpin and the other by the N-terminus of RECQ1, suggesting a non-hierarchical mechanism of tetramer assembly. Deletion of the β-hairpin leads to a dimeric structure were the two subunits are held together by the N-terminus (left), while deletion of the N-terminus leads to dimers held together by the β-hairpin mediated contacts (right).

The second patch (termed C2) involves an aromatic-rich loop in domain D1 which interacts with the same region in the other monomer. The β-hairpin of the WH domain (specifically, residues S560, F561, and T562 in one β-strand) forms a crucial part of the C3 patch. The tyrosine at the tip of the hairpin, Y564, is not however involved in protein:protein interactions, which is consistent with its proposed role in DNA strand separation.

Detailed mutational analysis confirmed the important role of the β-hairpin in dimer formation. Deletions that shorten the hairpin, or substitute the interacting residues with alanines in RECQ1^{T1} cause the mutant proteins to purify exclusively as monomers (Figures 2 and 4A). The second region involved in dimer interaction (C2) includes an aromatic-rich loop in domain D1 that interacts with the same region in the other monomer. In contrast with

the β-hairpin mutations, the substitution to Ala of two key residues of this loop, W227 and F231, is not sufficient to abrogate dimer formation. This could be due to the fact that the mutations of residues in the C2 region only disrupt one of the three patches involved in dimer formation, while mutations in the β-hairpin module simultaneously perturb two of the contacts involved in the 'head-to-tail' dimer interface. However, additional mutations in C2 region would be required to confirm this hypothesis. Of note, the aromatic-rich of region C2 was previously identified by Keck and co-workers as essential for DNA-coupled ATP hydrolysis (31). Consistently, we found that the W227A-F231A mutant of RECQ1 is unable to unwind DNA, although it retains the ability to bind DNA. Interestingly, this aromatic loop includes the highly conserved sequence CxSQWGHDFR which is characteristic of RecQ helicases—but is not present in other helicases of the SF-1 and SF-2 family—suggesting that it may present a unique aspect of the catalytic mechanism of RecQ helicases (37).

While RECQ1 is able to form dimers, the bacterial RecQ is a monomer in solution and does not exhibit a clear dimer interface in the crystal. Indeed, the different orientation of the WH domain, and the poor conservation of many of the residues involved in the dimer contact, seems to preclude a similar dimeric association. At this point, we can only speculate on the functional significance of the dimeric structure of RECQ1. To assess the functional significance of the dimerization of $RECQ1^{T1}$, one needs to examine the activity of mutants that are unable to form dimers. The mutants affecting the dimeric state are alterations of the β-hairpin, which is now seen to have two functions (disruption of the DNA duplex and protein:protein interaction). To disentangle these two effects, we tested the DNA unwinding activity, the DNA binding properties and oligomeric state of several mutants, which are summarized in Table 4. The single substitution of the aromatic Y564 to Ala abolishes DNA unwinding, but does not affect DNA binding and dimer formation. Conversely, mutants in which the hairpin is shortened (Δ561–562–566) or substituted (AAA:559–560–561) without changing Y564, fail to form stable dimers, but are at least partially active in DNA unwinding. Interestingly, this reduced DNA unwinding activity is associated to a weaker DNA binding affinity of these mutants for the fork DNA duplexes. Thus, we conclude that dimerization is not essential for helicase activity, although it may regulate the efficiency of DNA unwinding by providing an additional interface that stabilizes the RECQ1–DNA complex. The relative activity of monomers and higher multimers of non-hexameric helicases has been the subject of some debate (38). Previous studies suggested that some helicases, such as the *Escherichia coli* Rep and UvrD helicases, need to oligomerize in order to achieve full DNA unwinding activity (39,40). The mode of cooperation of multiple helicases acting on a single substrate is not clear. It is likely that only one helicase molecule contacts the strand separation point, while the additional molecules tug on the 3′-ssDNA tail, increasing the force or processivity or preventing slippage. The stable dimeric structure of RECQ1 may be important in this context. The helicase domains of other RecQ-family proteins exist as monomers (22,41–43). Compared with these helicases, RECQ1 lacks the C-terminal HRDC domain, which is thought to play a role in DNA binding in other RecQ-family helicases. Thus, one could speculate that the dimerization of RECQ1 provides an additional DNA binding interface that is normally provided by the HRDC domain. On the other hand, some of the proposed functions of the HRDC domain of other RecQ helicases, such as HJ recognition (44–46), might not be simply 'rescued' by dimerization since none of truncated $RECQ1^{T1}$ protein variants binds or unwinds HJ, independently on whether they form dimers or not (Table 4) (20).

The full-length RECQ1 exists in two oligomeric forms: a higher order oligomeric form which we here identify as a tetramer, and a smaller form which is a dimer. However, the fact that a deletion mutant lacking eight residues on both strands of the β-hairpin in addition to the Y564A substitution (Δ8-Y564A-$RECQ1^{FL}$) in the full-length context still forms dimers suggests that the tetramers observed in the full-length contexts are not simply a 'dimer of dimers'. Rather, tetramers are formed by two independent protein–protein contacts, one mediated by the C1–C3 contact, as we see in the crystal structure of the truncated protein, and another mediated by the N-terminus of RECQ1, as suggested from our previous size exclusion chromatography analysis of truncated versions of the protein lacking the first 48 or 56 residues (20,21). These results were also confirmed by GST pull-down assays showing that oligomer assembly is indeed mediated by the N-terminus and a C-terminal domain containing the β-hairpin (Figure 7). Thus, we can elaborate a model for tetramer formation that is not hierarchical: a protein interaction surface represented by the N-terminus of RECQ1, which normally mediates tetramer formation, is still functional in the (Δ8-Y564A-$RECQ1^{FL}$) mutant and might hold the two subunits together even though they lack their basic dimer interface (Figure 8).

In summary, this study provides novel information on the structural determinants and the oligomeric forms of RECQ1 associated with DNA unwinding as well as on the mechanism that regulates higher assembly state formation. We show that the β-hairpin module is not only crucial for the DNA strand separation activity of RECQ1, but it is also essential to mediate dimer formation in the context of the truncated protein and tetramer formation in the context of full-length RECQ1. Interestingly, dimer formation promotes DNA unwinding, while tetramer formation seems to be required for more specialized activities. However, many questions remain. First, does the β-hairpin module work as a 'pin' to separate the complementary strands and as a 'module' to promote oligomer formation, in all RecQ helicases? Our mutagenesis studies suggest that this is not the case. When we compared the helicase activity of the β-hairpin mutants of RECQ1 and *E. coli* RecQ, we clearly saw that mutations in the β-hairpin of the bacterial protein did not have an impact on the helicase activity of *E. coli* RecQ

(21). Moreover, *E. coli* RecQ is monomeric, suggesting that RecQ helicases might adopt different mechanisms and oligomeric structures to promote DNA unwinding (22,42). Second, what is the functional significance of the higher order oligomeric structures observed for several RecQ helicases? Our previous studies with the N-terminally deleted RECQ1 mutants indicated that these mutants were unable to resolve HJ structures or to promote the annealing of complementary ssDNA duplexes, suggesting that higher order oligomers are required for more 'specialized' activities. This notion is also supported by the previous observation made for BLM and WRN that connected their strand annealing activity to the ability to form higher order protein–DNA complexes (47,48). However, further work will be required to test the role of the β-hairpin module in other RecQ helicases and define the exact stoichiometry and functions of these higher order RecQ helicase complexes. These future studies will contribute to explain the distinct functions of the various RecQ helicase homologs present in eukaryotes and might shed light on how the lack of one or more of these 'specialized' RecQ helicase activities are linked to increased genomic instability and tumorigenesis.

ACKNOWLEDGEMENTS

The contribution of Drs Silvia Costantini, Venkateswarlu Popuri and Gianluca Triolo in providing the necessary guidelines for protein production and biochemical assays is gratefully acknowledged.

FUNDING

Associazione Italiana per la Ricerca sul Cancro (AIRC; AIRC5088 to A.V.); Structural Genomics Consortium is a registered charity (number 1097737) that receives funds from the Canadian Institutes for Health Research; the Canadian Foundation for Innovation; Genome Canada through the Ontario Genomics Institute; GlaxoSmithKline; Karolinska Institutet; the Knut and Alice Wallenberg Foundation; the Ontario Innovation Trust; the Ontario Ministry for Research and Innovation; Merck & Co., Inc.; the Novartis Research Foundation; the Swedish Agency for Innovation Systems; the Swedish Foundation for Strategic Research; the Wellcome Trust. Funding for open access charge: Associazione Italiana per la Ricerca sul Cancro (AIRC; AIRC5088).

Conflict of interest statement. None declared.

REFERENCES

1. Nakayama,H., Nakayama,K., Nakayama,R., Irino,N., Nakayama,Y. and Hanawalt,P.C. (1984) Isolation and genetic characterization of a thymineless death-resistant mutant of Escherichia coli K12: identification of a new mutation (recQ1) that blocks the RecF recombination pathway. *Mol. Gen. Genet.*, **195**, 474–480.
2. Bohr,V.A. (2008) Rising from the RecQ-age: the role of human RecQ helicases in genome maintenance. *Trends Biochem Sci.*, **33**, 609–620.
3. Chu,W.K. and Hickson,I.D. (2009) RecQ helicases: multifunctional genome caretakers. *Nat. Rev. Cancer*, **9**, 644–654.
4. Hartung,F. and Puchta,H. (2006) The RecQ gene family in plants. *J. Plant Physiol.*, **163**, 287–296.
5. Ellis,N.A., Groden,J., Ye,T.Z., Straughen,J., Lennon,D.J., Ciocci,S., Proytcheva,M. and German,J. (1995) The Bloom's syndrome gene product is homologous to RecQ helicases. *Cell*, **83**, 655–666.
6. Kitao,S., Lindor,N.M., Shiratori,M., Furuichi,Y. and Shimamoto,A. (1999) Rothmund-thomson syndrome responsible gene, RECQL4: genomic structure and products. *Genomics*, **61**, 268–276.
7. Siitonen,H.A., Kopra,O., Kaariainen,H., Haravuori,H., Winter,R.M., Saamanen,A.M., Peltonen,L. and Kestila,M. (2003) Molecular defect of RAPADILINO syndrome expands the phenotype spectrum of RECQL diseases. *Hum. Mol. Genet.*, **12**, 2837–2844.
8. Van Maldergem,L., Siitonen,H.A., Jalkh,N., Chouery,E., De Roy,M., Delague,V., Muenke,M., Jabs,E.W., Cai,J., Wang,L.L. *et al.* (2006) Revisiting the craniosynostosis-radial ray hypoplasia association: Baller-Gerold syndrome caused by mutations in the RECQL4 gene. *J. Med. Genet.*, **43**, 148–152.
9. Yu,C.E., Oshima,J., Fu,Y.H., Wijsman,E.M., Hisama,F., Alisch,R., Matthews,S., Nakura,J., Miki,T., Ouais,S. *et al.* (1996) Positional cloning of the Werner's syndrome gene. *Science*, **272**, 258–262.
10. Li,D., Frazier,M., Evans,D.B., Hess,K.R., Crane,C.H., Jiao,L. and Abbruzzese,J.L. (2006) Single nucleotide polymorphisms of RecQ1, RAD54L, and ATM genes are associated with reduced survival of pancreatic cancer. *J. Clin. Oncol.*, **24**, 1720–1728.
11. Futami,K., Kumagai,E., Makino,H., Goto,H., Takagi,M., Shimamoto,A. and Furuichi,Y. (2008) Induction of mitotic cell death in cancer cells by small interference RNA suppressing the expression of RecQL1 helicase. *Cancer Sci.*, **99**, 71–80.
12. Futami,K., Kumagai,E., Makino,H., Sato,A., Takagi,M., Shimamoto,A. and Furuichi,Y. (2008) Anticancer activity of RecQL1 helicase siRNA in mouse xenograft models. *Cancer Sci.*, **99**, 1227–1236.
13. Futami,K., Ogasawara,S., Goto,H., Yano,H. and Furuichi,Y. RecQL1 DNA repair helicase: a potential tumor marker and therapeutic target against hepatocellular carcinoma. *Int. J. Mol. Med.*, **25**, 537–545.
14. Bachrati,C.Z. and Hickson,I.D. (2003) RecQ helicases: suppressors of tumorigenesis and premature aging. *Biochem. J.*, **374**, 577–606.
15. Bachrati,C.Z. and Hickson,I.D. (2008) RecQ helicases: guardian angels of the DNA replication fork. *Chromosoma*, **117**, 219–233.
16. Bennett,R.J. and Keck,J.L. (2004) Structure and function of RecQ DNA helicases. *Crit. Rev. Biochem. Mol. Biol.*, **39**, 79–97.
17. Opresko,P.L., Cheng,W.H. and Bohr,V.A. (2004) Junction of RecQ helicase biochemistry and human disease. *J. Biol. Chem.*, **279**, 18099–18102.
18. Ouyang,K.J., Woo,L.L. and Ellis,N.A. (2008) Homologous recombination and maintenance of genome integrity: cancer and aging through the prism of human RecQ helicases. *Mech. Ageing Dev.*, **129**, 425–440.
19. Seki,M., Yanagisawa,J., Kohda,T., Sonoyama,T., Ui,M. and Enomoto,T. (1994) Purification of two DNA-dependent adenosinetriphosphatases having DNA helicase activity from HeLa cells and comparison of the properties of the two enzymes. *J. Biochem.*, **115**, 523–531.
20. Popuri,V., Bachrati,C.Z., Muzzolini,L., Mosedale,G., Costantini,S., Giacomini,E., Hickson,I.D. and Vindigni,A. (2008) The Human RecQ helicases, BLM and RECQ1, display distinct DNA substrate specificities. *J. Biol. Chem.*, **283**, 17766–17776.
21. Pike,A.C., Shrestha,B., Popuri,V., Burgess-Brown,N., Muzzolini,L., Costantini,S., Vindigni,A. and Gileadi,O. (2009) Structure of the human RECQ1 helicase reveals a putative strand-separation pin. *Proc. Natl Acad. Sci. USA*, **106**, 1039–1044.

22. Bernstein,D.A., Zittel,M.C. and Keck,J.L. (2003) High-resolution structure of the E.coli RecQ helicase catalytic core. *EMBO J.*, **22**, 4910–4921.
23. Muzzolini,L., Beuron,F., Patwardhan,A., Popuri,V., Cui,S., Niccolini,B., Rappas,M., Freemont,P.S. and Vindigni,A. (2007) Different quaternary structures of human RECQ1 are associated with its dual enzymatic activity. *PLoS Biol.*, **5**, e20.
24. Vindigni,A. and Hickson,I.D. (2009) RecQ helicases: multiple structures for multiple functions? *HFSP J.*, **3**, 153–164.
25. Buttner,K., Nehring,S. and Hopfner,K.P. (2007) Structural basis for DNA duplex separation by a superfamily-2 helicase. *Nat. Struct. Mol. Biol.*, **14**, 647–652.
26. Cui,S., Arosio,D., Doherty,K.M., Brosh,R.M. Jr, Falaschi,A. and Vindigni,A. (2004) Analysis of the unwinding activity of the dimeric RECQ1 helicase in the presence of human replication protein A. *Nucleic Acids Res.*, **32**, 2158–2170.
27. Brown,P.H. and Schuck,P. (2006) Macromolecular size-and-shape distributions by sedimentation velocity analytical ultracentrifugation. *Biophys. J.*, **90**, 4651–4661.
28. Paolinelli,R., Mendoza-Maldonado,R., Cereseto,A. and Giacca,M. (2009) Acetylation by GCN5 regulates CDC6 phosphorylation in the S phase of the cell cycle. *Nat. Struct. Mol. Biol.*, **16**, 412–420.
29. Marcello,A., Massimi,P., Banks,L. and Giacca,M. (2000) Adeno-associated virus type 2 rep protein inhibits human papillomavirus type 16 E2 recruitment of the transcriptional coactivator p300. *J. Virol.*, **74**, 9090–9098.
30. Krissinel,E. and Henrick,K. (2007) Inference of macromolecular assemblies from crystalline state. *J. Mol. Biol.*, **372**, 774–797.
31. Zittel,M.C. and Keck,J.L. (2005) Coupling DNA-binding and ATP hydrolysis in Escherichia coli RecQ: role of a highly conserved aromatic-rich sequence. *Nucleic Acids Res.*, **33**, 6982–6991.
32. Singleton,M.R., Dillingham,M.S. and Wigley,D.B. (2007) Structure and mechanism of helicases and nucleic acid translocases. *Annu. Rev. Biochem.*, **76**, 23–50.
33. Kitano,K., Kim,S.Y. and Hakoshima,T. Structural basis for DNA strand separation by the unconventional winged-helix domain of RecQ helicase WRN. *Structure*, **18**, 177–187.
34. Lee,J.Y. and Yang,W. (2006) UvrD helicase unwinds DNA one base pair at a time by a two-part power stroke. *Cell*, **127**, 1349–1360.
35. Velankar,S.S., Soultanas,P., Dillingham,M.S., Subramanya,H.S. and Wigley,D.B. (1999) Crystal structures of complexes of PcrA DNA helicase with a DNA substrate indicate an inchworm mechanism. *Cell*, **97**, 75–84.
36. Kim,J.L., Morgenstern,K.A., Griffith,J.P., Dwyer,M.D., Thomson,J.A., Murcko,M.A., Lin,C. and Caron,P.R. (1998) Hepatitis C virus NS3 RNA helicase domain with a bound oligonucleotide: the crystal structure provides insights into the mode of unwinding. *Structure*, **6**, 89–100.
37. Vindigni,A., Marino,F. and Gileadi,O. (2010) Probing the structural basis of RecQ helicase function. *Biophys. Chem.*, **149**, 67–77.
38. Lohman,T.M., Tomko,E.J. and Wu,C.G. (2008) Non-hexameric DNA helicases and translocases: mechanisms and regulation. *Nat. Rev. Mol. Cell Biol.*, **9**, 391–401.
39. Ha,T., Rasnik,I., Cheng,W., Babcock,H.P., Gauss,G.H., Lohman,T.M. and Chu,S. (2002) Initiation and re-initiation of DNA unwinding by the Escherichia coli Rep helicase. *Nature*, **419**, 638–641.
40. Maluf,N.K., Fischer,C.J. and Lohman,T.M. (2003) A dimer of Escherichia coli UvrD is the active form of the helicase in vitro. *J. Mol. Biol.*, **325**, 913–935.
41. Janscak,P., Garcia,P.L., Hamburger,F., Makuta,Y., Shiraishi,K., Imai,Y., Ikeda,H. and Bickle,T.A. (2003) Characterization and mutational analysis of the RecQ core of the bloom syndrome protein. *J. Mol. Biol.*, **330**, 29–42.
42. Xu,H.Q., Deprez,E., Zhang,A.H., Tauc,P., Ladjimi,M.M., Brochon,J.C., Auclair,C. and Xi,X.G. (2003) The Escherichia coli RecQ helicase functions as a monomer. *J. Biol. Chem.*, **278**, 34925–34933.
43. Zhang,X.D., Dou,S.X., Xie,P., Hu,J.S., Wang,P.Y. and Xi,X.G. (2006) Escherichia coli RecQ is a rapid, efficient, and monomeric helicase. *J. Biol. Chem.*, **281**, 12655–12663.
44. Kim,Y.M. and Choi,B.S. (2010) Structure and function of the regulatory HRDC domain from human Bloom syndrome protein. *Nucleic Acids Res*, doi:10.1093/nar/gkq586.
45. von Kobbe,C., Thoma,N.H., Czyzewski,B.K., Pavletich,N.P. and Bohr,V.A. (2003) Werner syndrome protein contains three structure-specific DNA binding domains. *J. Biol. Chem.*, **278**, 52997–53006.
46. Wu,L., Chan,K.L., Ralf,C., Bernstein,D.A., Garcia,P.L., Bohr,V.A., Vindigni,A., Janscak,P., Keck,J.L. and Hickson,I.D. (2005) The HRDC domain of BLM is required for the dissolution of double Holliday junctions. *EMBO J.*, **24**, 2679–2687.
47. Cheok,C.F., Wu,L., Garcia,P.L., Janscak,P. and Hickson,I.D. (2005) The Bloom's syndrome helicase promotes the annealing of complementary single-stranded DNA. *Nucleic Acids Res*, **33**, 3932–3941.
48. Muftuoglu,M., Kulikowicz,T., Beck,G., Lee,J.W., Piotrowski,J. and Bohr,V.A. (2008) Intrinsic ssDNA annealing activity in the C-terminal region of WRN. *Biochemistry*, **47**, 10247–10254.